PROCEEDINGS OF THE INTERNATIONAL CONFERENCE NANOMATERIALS: APPLICATIONS AND PROPERTIES
Vol. 4 No 2, 02NNSA02(4pp) (2015)

Glutathione-Induced Release of Zeatin From Functionalized Gold Nanovectors

A. Zoppi[1,2], J.R. Molina-Contreras[3,*], P. Marsili[1,2], M. Muniz-Miranda[4], G. Margheri[2], S. Trigari[2], A. Leva[5], E. Giorgetti[2], F. Giammanco[1]

[1] *Physics Department, University of Pisa, Largo B. Pontecorvo 3,56127 Pisa, Italy*
[2] *ISC, CNR, Via Madonna del Piano 10, 50019 Sesto Fiorentino (FI), Italy*
[3] *Departamento de Ingeniería Eléctrica y Electrónica, Instituto Tecnológico de Aguascalientes, Av. Adolfo López Mateos No 1801 Ote., Fracc. Bona Gens, 20256, Aguascalientes, Ags, México*
[4] *Department of Chemistry, University of Firenze, Via della Lastruccia 3, 50019 Sesto Fiorentino (FI), Italy*
[5] *IVALSA, CNR, Via Madonna del Piano 10, 50019 Sesto Fiorentino (FI), Italy*

(Received 15 March 2015; published online 22 August 2015)

The paper shows our preliminary results on the different spectroscopic behavior of three types of gold nanoparticles (obtained respectively by chemical synthesis, laser ablation in pure water and laser ablation in a citrate solution) modified with trans-zeatin, a plant growth regulator, in presence of glutathione. The reaction of ligand substitution of the adsorbed zeatin with glutathione is studied through surface enhanced Raman spectroscopy and is revealed to occur only when citrate-laser ablated gold nanoparticles are employed, making these particles potentially good candidates as vehicles of zeatin inside plant cells for future agricultural applications.

Keywords: Zeatin, Glutathione, Gold Nanoparticles, Raman, SERS.

PACS numbers: 82.70.Dd, 87.14.Lk, 87.64.kp

1. INTRODUCTION

The number of applications in biosensors, sensors and biomedical diagnostics based on the interactions between nanoparticles and biologically relevant molecules, has attracted an increasing interest [1-4]. The study of model systems such amino acids or nucleic acids on well characterized nanoparticle-surfaces has represented a useful approach to developing an understanding of the structure and stability of bio-molecules formed at metal interfaces. In particular, Surface Enhanced Raman Scattering (SERS) turned to be a powerful investigation method for the detection of low analytical concentrations and for the identification of the conformation and orientation of molecules adsorbed on metal surfaces [5,6].

In this work we report our preliminary results on the studies of the capability of glutathione to induce the release of adsorbed zeatin from gold nanoparticles (AuNP), using SERS technique.

Zeatin, a derivative of purine, is a natural cytokinin which regulates multiple developmental and physiological processes in a plant through its ability to promote cell division, keep meristematic cell identity, maintain high cellular redox potentials during abiotic stress and regulate nutrient sink/source activity of different organs [7]. The chemical structure of zeatin is basically that of adenine whose SERS spectrum has been measured on both Ag and Au substrates [8-10]. Despite this cytokinin exists as cis- and trans-structures, only trans-zeatin (Fig. 1a) is biologically active and it is used in *in vitro* culture to stimulate the growth and the bud formation. However, due to its high cost, it is not recommended for large-scale subministrations.

Glutathione is a non enzymatic antioxidant which has a role in the defence mechanism and antioxidant capacity in plant under abiotic stress [11]. It is an important constituent of all living cells and the most abundant thiol species at a concentration range of 1−10 mM in the cytoplasm. It is a tripeptide made of glutamic acid, cysteine and glycine (Fig. 1b) where the –SH functionality is known to exhibit a strong affinity with metallic gold. For instance, this affinity has been already exploited for drug release from gold nanoparticles surfaces [12].

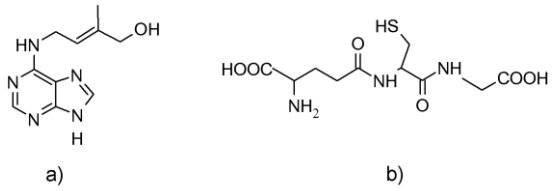

Fig. 1 – Chemical structures of: a) trans-zeatin and b) glutathione.

The basic idea is that glutathione, physiologically present in the cells, drives the release of zeatin molecules from hormone-labeled Au nanoparticles, thanks to its higher affinity for gold. Indeed, AuNP have been recently demonstrated to enter and accumulate in plant cells with very low or none toxicity [13, 14]. In this respect, AuNP could offer an efficient tool for the loading and transportation of zeatin inside plant cells, where it can be freed by glutathione exchange. Zeatin-enriched gold nanoparticles could be thus employed as novel vectors that can potentially deliver a higher amount of phytohormones, reducing costs in plants growth procedures, like for instance in commercial micropropagation protocols.

To check the ability of glutathione to induce a lig-

* jrmolinacon@gmail.com

and-exchange reaction on zeatin-labeled Au nanoparticles, three different gold aqueous colloidal suspensions were tested: *AuNP_chem* was obtained by chemical reduction of gold ions with sodium citrate, *AuNP_abl* was prepared by laser ablation in pure water and *AuNP_citr_abl* was obtained by laser ablation in a citrate solution. The colloidal suspensions were modified with zeatin and glutathione addition was inspected through Raman measurements.

We found that ligand exchange occurred only with *AuNP_citr_abl* and we believe that these results could be useful for the understanding of complex biological systems opening the way to applications in plant science, agriculture and biotechnology.

2. EXPERIMENTAL

2.1 Sample preparation

AuNP_chem was prepared by Na-citrate reduction of $HAuCl_4$ according to the modified Turkevitch method [15].

Laser ablation was performed by irradiating a gold target with the fundamental wavelength (1064 nm) of a Q-switched Nd:YAG laser (rep. rate 10 Hz, pulse width 17 ns) with 220 mJ pulse energy. The laser was focused on the target in order to obtain a circular spot of 1.5 mm, corresponding to a 124 mJ/mm^2 fluence. *AuNP_abl* was prepared in pure water while *AuNP_citr_abl* was obtained in a 10^{-4} M Na-citrate solution.

Trans-zeatin was used as an alkaline solution (pH 12), glutathione was dissolved in pure water. Ultrapure water (18.2 MΩ·cm @ 25°C) was used for all preparations.

2.2 Methods

Extinction spectra were obtained at room temperature using a Cary 5 spectrometer in quartz cuvettes.

Raman spectra were recorded at room temperature using a single grating RM2000 Renishaw micro-Raman apparatus with an air cooled, charge coupled device and coupled with a near IR laser diode emitting at 785 nm. Raman spectra were taken on a dried drop of the colloidal suspension put on an aluminium foil. A 20x magnification objective was used to probe the drop in several points.

FT-SERS spectra were recorded using a Multi-Raman (Bruker) apparatus operating at 1064 nm and coupled to a liquid-N_2 cooled Ge detector. Irradiation power and spectral resolution were respectively set at 500 mW and 4 cm^{-1}. A 10 mm glass cuvette was used to record the spectra of 0.5 ml of the suspensions, averaging over 200 scans.

In order to check the glutathione-induced release of zeatin from gold nanoparticles, the colloidal concentrations were previously adjusted to a 0.8 extinction maximum (optical path 2 mm). Zeatin was added to the colloidal suspension to a final concentration of 10^{-5} M (pH 4-5) and spectral characterization was performed after ten minutes. The effect of 10^{-3} M glutathione was then checked. This value of concentration was selected according to the glutathione level in living cells.

3. RESULTS AND DISCUSSION

3.1 AuNP_chem colloidal suspension

The citrate-reduced AuNP colloid was very sensitive to the addition of 10^{-5} M zeatin. This was macroscopically evidenced by the colour changes of the suspension. Fig. 2 compares the extinction spectrum of the pure colloid with those acquired on zeatin@*AuNP_chem* for different cytokinin concentrations. As evidenced, zeatin addition caused a flattening of the main plasmonic band at 526 nm, that is characteristic of spherical particles, while a new band appears and becomes prominent in the 750-800 nm spectral range, attributable to nanoparticle aggregation. Besides, the absorption peak of zeatin occurs at 270 nm.

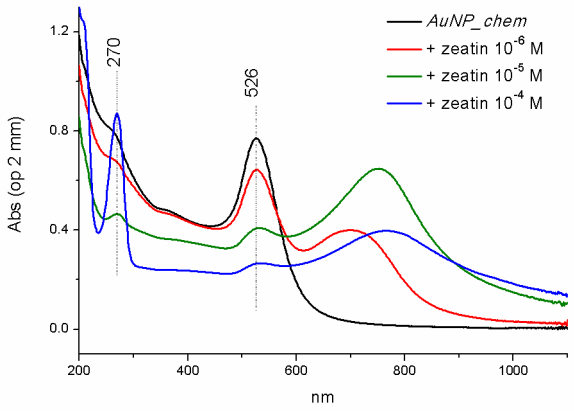

Fig. 2 – UV-vis spectra of the *Au_NP_chem* colloidal suspension before and after the addition of zeatin 10^{-6} M, 10^{-5} M, 10^{-4} M. The absorption peak at 270 nm is attributed to the cytokinin molecule.

The SERS spectra of zeatin at 10^{-4}, 10^{-5} and 10^{-6} M concentrations were then taken on dried drops. Fig. 3 compares three typical SERS spectra with the Raman spectrum taken on an aqueous solution of zeatin.

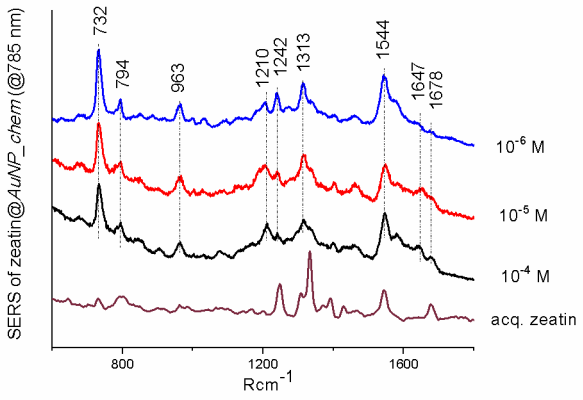

Fig. 3 - SERS spectra (@785 nm) of zeatin@*AuNP_chem* colloid at different concentrations of the cytokinin, compared with the observed Raman spectrum of a 2×10^{-2} M solution of zeatin (pH 12).

With respect to free zeatin, SERS spectra show an intensification of the 732 cm^{-1} band which can be associated to the purine ring breathing mode, as already predicted for SERS spectra of adenine measured on gold [8,9]. Other signals are enhanced such as those

near 1210 cm^{-1} and 1310 cm^{-1}. On the whole, chemically reduced gold NPs behave as a good SERS substrate for the detection of zeatin giving a fair reproducibility of the measured spectra.

Due to the quite large red shift of the extinction maximum observed as a consequence of the addition of zeatin, FT-SERS spectra were also collected for 10^{-5} and 10^{-6} M zeatin (Fig 4). This method had moreover the advantage of making the measurements directly on the colloidal solution which allowed us to check immediately the effect of glutathione as well. 10^{-3} M glutathione was tested for the 10^{-6} M zeatin@*AuNP_chem* sample. Despite the 1000:1 ratio, glutathione resulted to be ineffective, suggesting a very strong linkage of zeatin molecules to the gold surface. The measured spectrum in fact remained unchanged even one day later.

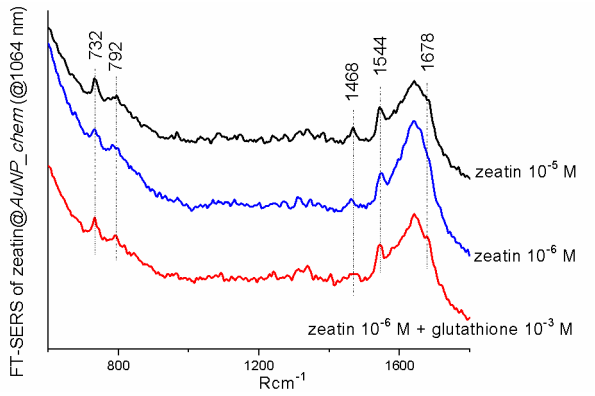

Fig. 4 – FT-SERS (@1064 nm) spectra of zeatin in 10^{-5} M and 10^{-6} M concentrations, adsorbed on *AuNP_chem*. Effect of 10^{-3} M glutathione addition to 10^{-6} M zeatin@*AuNP_chem*.

3.2 AuNP_abl colloidal suspension

According to the previous results, we considered a different type of colloid to be used as zeatin carrier. In particular we used AuNP prepared through laser ablation in pure water. With respect to chemical reduction procedures, laser ablation offers the highest purity and a surfactant-free surface, which allows for example effective and non mediated interaction of the metal with the environment. Moreover, the "naked" AuNPs exhibit an excellent stability and in general a monomodal and monodisperse size distribution [16] which may be a challenge with traditional chemical procedures.

The plasmonic band of *AuNP_abl* suspension was peaked at 522 nm and was less sensitive to zeatin addition with respect to the chemically citrate reduced sample discussed before. 10^{-5} M zeatin did not produce any significant spectral shift of the plasmonic band, while a small widening was observed after the addition of glutathione (Fig. 5). Despite the assembly of gold nanoparticles mediated by glutathione has been already reported [17], we did not observe this effect on the naked nanoparticles.

The scarce reactivity of *AuNP_abl* towards zeatin anchorage was further confirmed spectroscopically. The Raman spectra appeared very poorly enhanced by the metallic substrate. The effect of glutathione addition was thus not revealed (Fig. 6).

3.3 AuNP_citr_abl colloidal suspension

The same procedure of laser ablation was repeated in a 10^{-4} M Na-citrate solution to prepare *AuNP_citr_abl* nanoparticles.

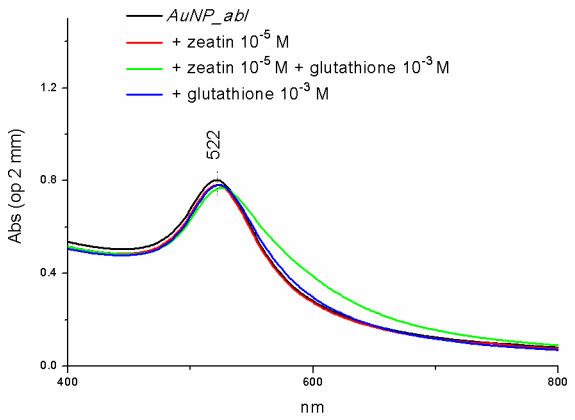

Fig. 5 – UV-vis spectra of *AuNP_abl*, before and after the addition of 10^{-5} M zeatin and 10^{-3} M glutathione.

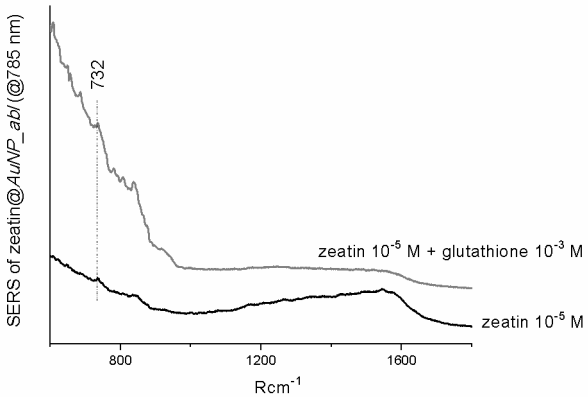

Fig. 6 – Representative SERS spectrum of zeatin@*AuNP_abl* before and after addition of glutathione (zeatin 10^{-5} M, glutathione 10^{-3} M).

The plasmonic band, centred at 517 nm, moved to 520 nm after the addition of 10^{-5} M zeatin and shifted to 620 nm after glutathione addition (Fig. 7). Glutathione promoted the assembly of not-labelled nanoparticles as well.

Moreover, zeatin gave strong SERS signals, which disappeared after the addition of glutathione, attesting a strong cleavage effect (Fig. 8).

The occurrence of an interaction between gold surface and the ligand molecules was apparently favoured by the presence of citrate ions. This could be tentatively correlated to the mild reducing properties of citrate ions as they kept gold surface free from oxidised species not available for the ligand adsorption. This is even better evidenced by comparing the free-zeatin absorption peaks measured before and after glutathione addition. Fig. 9a shows that a higher ligand adsorption occurs for *AuNP_citr_abl* in accordance with a higher reactivity of the nanoparticles surface. Besides, after glutathione addition, free-zeatin signal increases only for *AuNP_citr_abl*, due to the ligand-exchange reaction (Fig. 9b).

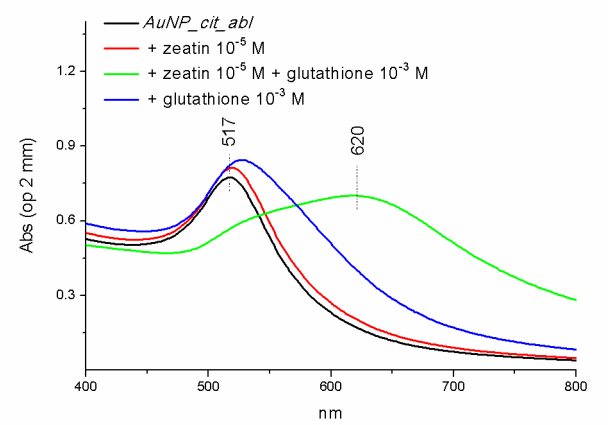

Fig. 7 – UV-vis spectra of *AuNP_citr_abl*, before and after the addition of 10^{-5} M zeatin and 10^{-3} M glutathione.

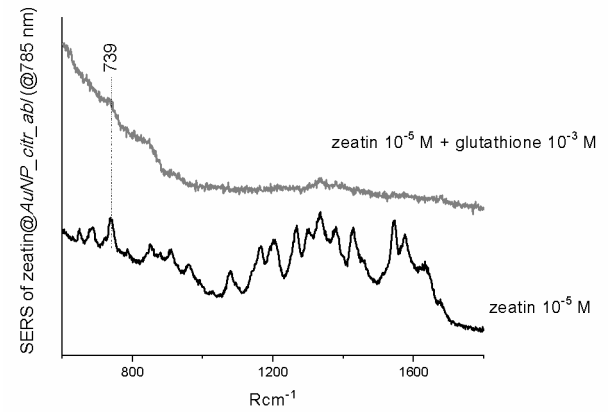

Fig. 8 – SERS spectra taken on zeatin@*AuNP_citr_abl*, before and after addition of glutathione (10^{-5} M zeatin, 10^{-3} M glutathione).

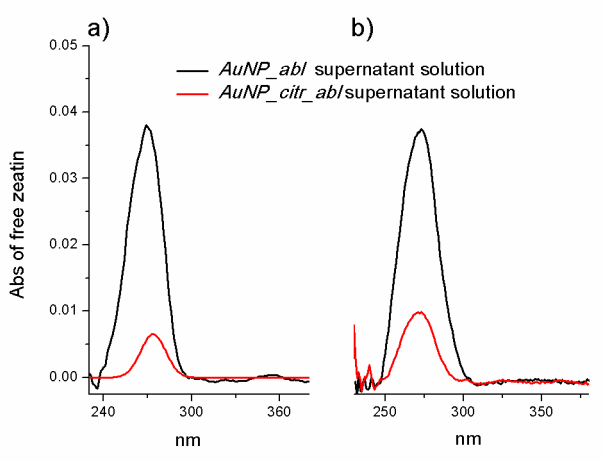

Fig. 9 – Comparison of the free-zeatin absorption peak (measured in the supernatant solution) before (a) and after (b) addition of 10^{-3} M glutathione to *AuNP_abl* and *AuNP_citr_abl* colloidal suspensions with 10^{-5} M zeatin.

Coming to the conclusions of this work, we found that glutathione-induced release of zeatin occurred solely on citrate-laser-ablated nanoparticles. At this stage we are not able to explain other questions, such as why *AuNP_chem* behaved differently. This aspect is set aside for future developments.

REFERENCES

1. W. Russ Algar, D.E. Prasuhn, M.H. Stewart, T.L. Jennings, J.B. Blanco-Canosa, P.E. Dawson, I.L. Medintz, *Bioconjugate Chem*. **22**, 825 (2011).
2. R.A. Sperling, W.J. Parak, *Phil. Trans. R. Soc. A* **368**, 1333 (2010).
3. Y. Wang, B. Yan, L. Chen, *Chem. Rev.* **113**, 1391 (2013).
4. C. Kim, E.C. Cho, J. Chen, K.H. Song, L. Au, C. Favazza, Q. Zhang, C.M. Cobley, F. Gao, Y. Xia, L.V. Wang, *ACS Nano* **4** No8, 4559 (2010).
5. S.E.J. Bell, N.M.S. Sirimuthu, *J. Am. Chem. Soc.* **128**, 15580 (2006).
6. J.S. Suh, M. Moskovits, *J. Am. Chem. Soc.* **108**, 4711 (1986).
7. D. Zalabák, H. Pospíšilová, M. Šmehilová, K. Mrízová, I. Frébort, P. Galuszka, *Biotechnol. Adv.* **31**, 97 (2013).
8. M. Pagliai, S. Caporali, M. Muniz-Miranda, G. Pratesi, V. Schettino, *J. Phys. Chem. Lett.* **3**, 242 (2012).
9. J. Kundu, O. Neumann, B.G. Janesko, D. Zhang, S. Lal, A. Barhoumi, G.E. Scuseria, N.J. Halas, *J. Phys. Chem. C* **113**, 14390 (2009).
10. M. Muniz-Miranda, C. Gellini, M. Pagliai, M. Innocenti, P.R. Salvi, V. Schettino, *J. Phys. Chem. C* **114**, 13730 (2010).
11. G. Noctor, A. Mhamdi, S. Chaouch, Y. Han, J. Neukermans, B. Marquez-Garcia, G. Queval, C.H. Foyer, *Plant Cell Environ.* **35**, 454 (2012).
12. K. Ock, W.I. Jeon, E.O. Ganbold, M. Kim, J. Park, J.H. Seo, K. Cho, S.W. Joo, S.Y. Lee, *Anal. Chem.* **84**, 2172 (2012).
13. I. Kokinaa, V. Gerbredersb, E. Sledevskisb, A. Bulanovsb, *J. Biotechnol.* **165**, 127 (2013).
14. G. Zhai, K.S. Walters, D.W. Peate, P.J.J. Alvarez, J. L. Schnoor, *Environ. Sci. Technol. Lett.* **1**, 146 (2014).
15. J. Kimling, M. Maier, B. Okenve, V. Kotaidis, H. Ballot, A. Plech, *J. Phys. Chem. B* **110**, 15700 (2006).
16. M. Muniz-Miranda, C. Gellini, E. Giorgetti, G. Margheri, P. Marsili, L. Lascialfari, L. Becucci, S. Trigari, F. Giammanco, *Thin Solid Films* **543**, 118 (2013).
17. I.S. Lim, D. Mott, W. Ip, P.N. Njoki, Y. Pan, S. Zhou, C.J. Zhong, *Langmuir* **24**, 8857 (2008).